Research Article

Modeling and Analysis of Photo-Voltaic Solar Panel under Constant Electric Load

Elias M. Salilih [1] and Yilma T. Birhane[2]

[1]*Department of Mechanical Engineering, Jigjiga university, PO Box 1020, Jigjiga, Ethiopia*
[2]*School of Mechanical & Industrial Engineering, A.A. Institute of Technology-AAU, Ethiopia*

Correspondence should be addressed to Elias M. Salilih; elju99@gmail.com

This paper presents modelling electrical performance of a typical PV panel/module (which is Kyocera 200GT) for constant electric loads (which are 2Ω, 4Ω, 6Ω, and 8Ω) under weather condition of a tropical region. The specific case of the city Jigjiga (9.35°N,42.8°E), located in the Eastern region of Ethiopia is considered. Electrical characteristics of the PV module are determined on the basis of detailed numerical algorithm, which was designed based on tested numerical technique from reviewed articles. The overall evaluation of the hourly variation in the electrical performance of the PV module is done by means of graphical technique, which determines the operating point of the PV module on voltage vs. current plane for each load, and the performance of the PV panel is compared for each load. The 4Ω electric load resulted in highest daily energy output of the PV panel on a daily basis for 11 days of the month of January (out of 12 considered days), but in the last day it resulted in a poorer performance with respect to the other two electrical loads (i.e., 6Ω and 8Ω electric loads).

1. Introduction

Renewable energy systems have a significant advantage on the ecology, economy, and political matters of the world [1]. It is estimated that renewable energy sources could account for three fifths of the world's electricity market share and two fifths of the market for fuels by the middle of the 21st century. Moreover, shifting to a renewable energy economy will result in significant environmental and other advantages which are not quantified in economic terms.

It is predicted that by 2050 carbon dioxide (CO_2) emissions of the world will be reduced to 75% of their 1985 levels, which will as a result of efficient use of energy and wide adoption of renewable energy usage [2].

Solar renewable energy systems are more environmentally friendly than conventional energy sources over electricity generation. The advantages of using solar energy systems fall into two main categories: ecology and socioeconomic issues. From an ecological aspect, the use of solar energy technologies has various positive impacts that include reduction of greenhouse gas emissions (like CO_2, NO_x) and

of toxic gas emissions (SO_2, particulates), prevention of soil pollution, reduction of transmission cost, and improvement in the quality of water resources [3–8]. The advantages of solar technologies comprise energy independency, employment opportunity creation [4, 5], acceleration of electrification of rural communities in isolated areas, and diversification and security (stability) of energy supply [4, 5, 9].

Photovoltaic systems sometimes called solar cells have found widespread application because they are simple, are compact, and have high power-to-weight ratio [10]. PV cell behaves more like a current source than a voltage source. Which means while the current output of the PV cell increases with an increase in solar insolation, the voltage output will remain constant irrespective to a variation in solar insolation [11], and this information is valuable in sizing PV panel for specific application.

The output characteristic of PV cell depends mainly on the solar insolation. Variations in solar irradiance and cell operating temperature will nonlinearly affect the current-voltage as well as power-voltage characteristics of a PV module [12]. In addition to the two parameters (i.e., solar

COUNTRY LOCATION MAP
ETHIOPIA

REGIONS OF ETHIOPA

- ADDIS ABABA
- AMHARA
- Afar
- BENISHANGUL-GUM
- DIRE DAWA
- GAMBELLA
- HARARI
- OROMIA
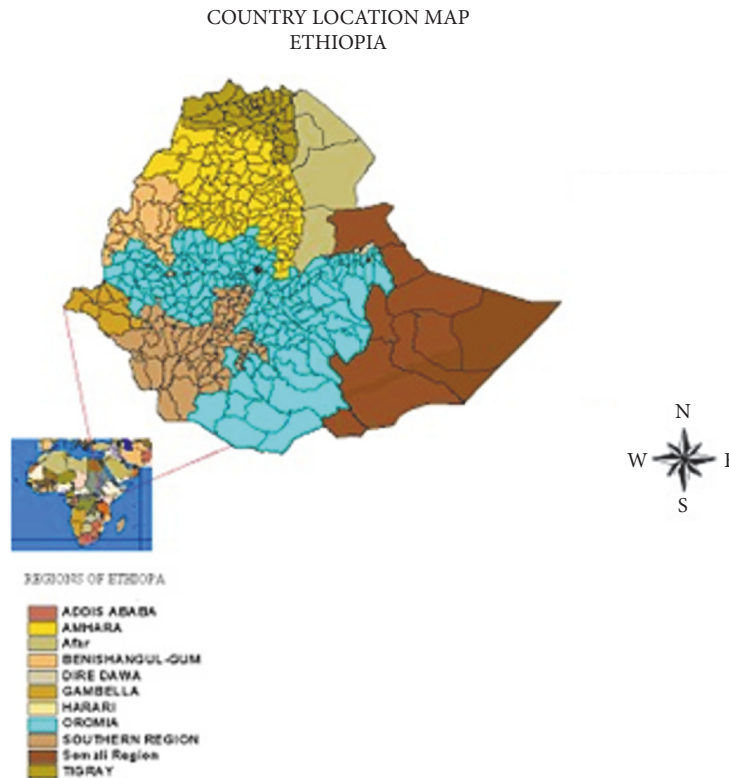- SOUTHERN REGION
- Somali Region
- TIGRAY

FIGURE 1: Location map of Ethiopia. Source Ministry of Agriculture, 2000.

irradiance and cell operating temperature), the performance of a PV module depends on its operating point on I-V plane. Forcing a PV module to operate near Maximum power point (MPP) results in a higher efficiency. Hence, in order to extract maximum power output from a PV module it can be controlled by maximum power point tracking (MPPT) controller [13]. MPPT controllers track maximum possible power from the Photovoltaic panel [14]. Thus, use of MPPT controller is one way of optimizing the performance of PV module.

Several research studies which focus on optimization of PV systems with the help of MPPT circuit have been conducted. Reshef et al. [15] investigated the optimization of solar array size with the MPPT controller for water pumping application. Singh et al. [16], Lujara et al. [17], and Ghoneim [18] studied the significance of MPPT controller on optimizing PV water pumping system. Veeresh S G et al. [19] modeled the optimization of a PV panel with MPPT controller which works with maximum conductance method. However, there is a research gap with regard to optimization of PV panel without MPPT controller. The research work in this paper is intended to fill this gap. This paper focuses on optimization of a PV panel with help of resistance matching technique.

In case of directly coupled PV system the electric load has an effect on the performance of the PV module. Perhaps, resistor matching technique is one way of optimizing performance of a PV module. In this research work, the effect of electrical load on efficiency of PV module was investigated. The aim of this research is to contribute to the optimum use of PV system by resistance or impedance matching technique. As it is known, some PV system can be directly coupled to PV panel; in those cases once the impedance of the load (such as an electric motor) is known, the technique which is demonstrated in this paper can be utilized to select a PV module for a particular load under specific weather condition. In this research, a particular PV panel/module Kyocera 200GT is simulated under weather condition of Jigjiga for various electric loads and which electric load performed well with the panel is investigated.

2. Study Area

The The Federal Democratic Republic of Ethiopia (FDRE) is a noncoastal country in east of Africa, surrounded to the north by Eritrea, to the west by Sudan, to the south by Kenya, and to the east by Somalia and Djibouti; it lies within the geographic coordinates from $3°24'$ North to $14°53'$ North and $32°42'$ East to $48°12'$ East (see Figure 1). It covers 1,120,000 square kilometers in nine regional states [20].

The study was carried out under weather condition of Jigjiga area located on 9.35° latitude and 42.8° longitude coordinate.

3. Modeling Characteristics of a PV Device

The objective of this section is to determine the detailed electrical characteristics of the PV panel/module from the
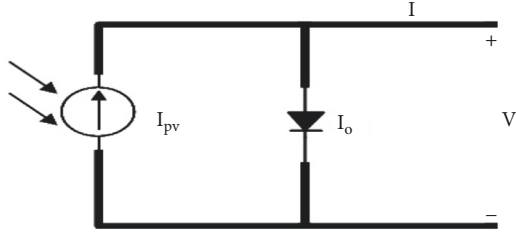
FIGURE 2: Simplified or Ideal equivalent circuit of a PV cell.
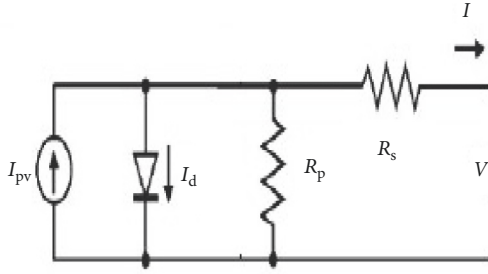

FIGURE 3: Single-diode model of the theoretical PV cell and equivalent circuit of a practical PV device including the series and parallel resistances.

manufacturer's specification, on current-voltage plane as well as on power-voltage plane, so that the output of the PV panel can be predicted under specific electrical loads.

3.1. IDEAL PV Cell. Figure 2 showed the equivalent circuit of a theoretical PV cell, while Figure 3 shows equivalent circuit of a practical PV device including the series and parallel resistances. And the basic equation from the theory of semiconductors that mathematically describes the I–V characteristic of the ideal PV cell is

$$I = I_{pv,cell} - I_{0,cell} \left[\exp\left(\frac{qV}{a\mathsf{K}T} \right) - 1 \right] \qquad (1)$$

$$I_d = I_0 \left[\exp\left(\frac{qV}{a\mathsf{K}T} \right) - 1 \right] \qquad (2)$$

where I_{pv} is the current generated by the incident light (it is directly proportional to the Sun irradiation), I_d is the Shockley diode equation, I_0 is the reverse saturation or leakage current of the diode, q is the electron charge ($1.60217646 \times 10^{-19}$ C), K is the Boltzmann constant ($1.3806503 \times 10^{-23}$ J/K), T (in Kelvin) is the temperature of the p–n junction, and a is the diode ideality constant.

3.2. Modeling the PV Module. All PV panel manufacturers provide basic electrical parameters about their product which are the voltage at the maximum power point (V_{mpp}), the nominal open-circuit voltage ($V_{oc,n}$), the nominal short-circuit current ($I_{sc,n}$), the current at maximum power point (I_{mpp}), temperature coefficient for the short-circuit current (K_I), temperature coefficient for the open-circuit voltage (K_V), and

the maximum power output ($P_{max,e}$). Those parameters are measured with reference to standard test conditions (STCs) of solar irradiation and cell temperature. The basic electrical parameters are not enough to investigate the performance of a PV panel. Hence, it is crucial to find out detailed electrical characteristics which model the performance of PV panel.

The basic equation (1) of the elementary PV cell does not determine the I–V characteristic of a practical PV module. Practical modules are made of several connected PV cells and the observation of the characteristics at the terminals of the PV modules requires the inclusion of additional parameters to the basic equation [21].

$$I = I_{pv} - I_0 \left[\exp\left(\frac{V + R_s I}{V_t a} \right) - 1 \right] - \frac{V + R_s I}{R_P} \qquad (3)$$

where I_{pv} and I_0 are the photovoltaic (PV) and saturation currents, respectively, of the modules and $V_t = N_s \mathsf{K}T/q$ is the thermal voltage of the modules with (N_s) number of cells connected in series.

The diode saturation current I_0 and its dependence on the temperature are expressed as [21]

$$I_0 = I_{0,n} \left(\frac{T_n}{T} \right)^3 \exp\left[\frac{qE_g}{a\mathsf{K}} \left(\frac{1}{T_n} - \frac{1}{T} \right) \right] \qquad (4)$$

where E_g is the band gap energy of the semiconductor ($E_g = 1.12$ eV for the polycrystalline Si at 25°C), $I_{0,n}$ is the nominal saturation current, and the value of diode ideality constant is usually between $1 \leq a \leq 1.5$ and for silicon-poly material it is around 1.3 [22]:

$$I_{0,n} = \frac{I_{sc,n}}{\exp\left(V_{oc,n}/aV_{t,n} \right) - 1} \qquad (5)$$

with $V_{t,n}$ being the thermal voltage of N_s series connected cells at the nominal temperature T_n.

The light-generated current of the PV cell depends linearly on the solar irradiation and is also influenced by the temperature according to the following equation [22]:

$$I_{pv} = \left(I_{Pv,n} + \mathsf{K}_I \Delta T \right) \frac{G}{G_n} \qquad (6)$$

where $I_{Pv,n}$ (in amperes) is the light-generated current at the nominal condition (usually 25°C and 1000 W/m^2), $\Delta T = T - T_n$ (T and T_n being the actual and nominal temperatures [in Kelvin], respectively), G (watts per square meters) is the irradiation on the device surface, and G_n is the nominal irradiation.

The nominal light-generated current $I_{Pv,n}$ can be expressed with accurate equation of the following [22].

$$I_{Pv,n} = \frac{R_P + R_S}{R_P} I_{sc,n} \qquad (7)$$

So, equation (3) can be expressed with the known values given by the manufacturer's data sheet ($I_{sc,n}$ and $V_{oc,n}$), the constants (a, q, E_g, K), and the external influential factors of

radiation and temperature (T, G), but the internal influencing parameters (R_s and R_p) are still unknown.

Marcelo G. et al. [21] proposed an interesting method for adjusting R_s and R_p based on the fact that there is only a pair $\{R_s, R_p\}$ which ensures $P_{max,m} = P_{max,e} = V_{mpp}I_{mpp}$ at the (V_{mpp}, I_{mpp}) point of the I–V curve; i.e., the maximum power computed by the I–V model of equation (3) ($P_{max,m}$) is equal to the maximum experimental power from the datasheet ($P_{max,e}$) at the MPP (where MPP is a maximum power point, which means a point where the power output of the solar panel will be maximum).

The calculated maximum current output of the solar panel at nominal temperature and solar radiation (at 25°C and 1000 W/m^2) could be expressed using (3) as

$$I_{mpp} = I_{pv,n} - I_{0,n}\left[\exp\left(\frac{V_{mpp} + R_s I_{mpp}}{V_{t,n}a}\right) - 1\right]$$
$$- \frac{V_{mpp} + R_s I_{mpp}}{R_P} \quad (8)$$

where V_{mpp} is voltage at MPP (maximum power point) and the thermal voltage of the modules at STC I_{mpp} is current at MPP.

Equation (8) is arranged in such a manner to express the shunt resistor with other variables as follows:

$$R_P$$
$$= \frac{V_{mpp} + R_s I_{mpp}}{I_{pv,n} - I_{0,n}\left[\exp\left((V_{mpp} + R_s I_{mpp})/V_{t,n}a\right) - 1\right] - I_{mpp}} \quad (9)$$

From (9) R_P is expressed not only in terms parameters such as $I_{pv,n}$, $I_{0,n}$, and $V_{t,n}$, but also in the nominal maximum power point (i.e. I_{mpp} and V_{mpp}) and the R_S; hence the resulting graph due to the pair values (i.e., R_S and R_P) will surely pass through the nominal maximum power points. With the help of the method which was proposed by *Marcelo G. et al.* [21], a detail numerical algorithm that can determine the electrical characteristic of a PV panel is designed, which is shown in Figure 4.

4. Operating Temperature and Efficiency of PV Module

According to the equations in Section 3 (see (3) to (7)); solar irradiance intensity (G) and cell operating temperature (T) are the two crucial parameters which nonlinearly affect the current-voltage as well as power-voltage characteristics of a PV module. In order to model the electrical characteristics of the PV module and its power output, first it is required to determine the cell operating temperature (T) of the PV module.

Standard heat transfer mechanics must be considered to calculate the energy balance on the cell module leading to the prediction of cell temperature. At steady-state conditions, only convection and radiation mechanisms are usually considered, since they are prevalent on the conduction mechanism that merely transports heat toward the surfaces of

the mounting frame (especially in the case of rack-mounting free-standing arrays). A survey of the explicit and implicit correlations proposed in literature linking cell temperature with standard weather variables and material and system-dependent properties [23].

A large number of empirical correlations exist in a number of literatures whose application appears to be the best and simplest. Hence, an equation has been chosen that is explicit, depends on easily measurable parameters and, has wide applicability. For variations in ambient temperature and irradiance the cell temperature (in °C) can be estimated quite accurately with the linear approximation [24]:

$$T = T_a + \frac{G}{G_{NOCT}}\left(T_{NOCT} - T_{a,NOCT}\right) \quad (10)$$

where T is the cell operating temperature of the PV module which determines the performance of the PV panel along with solar radiation intensity G and T_{NOCT} is nominal operating cell temperature which is a reference temperature for particular PV module to calculate cell operating temperature (T) and it is given by the manufacturer's specification. The nominal cell temperature (T_{NOCT}) is defined as the temperature of the cell at the conditions of the nominal terrestrial environment (NTE) [24]: Solar irradiance G_{NOCT}= 800 W/m^2, ambient temperature $T_{a,NOCT}$ = 20°C, and average wind speed 1 m/s. Hence equation (10) can be expressed as follows:

$$T = T_a + \frac{G}{800W/m^2}\left(T_{NOCT} - 20°\right) \quad (11)$$

The solar module power conversion efficiency can be given as

$$\eta = \frac{P_{out}}{G \times A_m} = \frac{I \times V}{G \times A_m} \quad (12)$$

where I and V are current and voltage output of the PV module corresponding to solar intensity G and cell temperature, T and A_m is solar panel module area (the dimension of KC200GT solar module can be found on manufacturer's spec.)

5. Methodology

A methodology implemented in this paper is a graphical technique, which is used to find an operating point of a PV panel.

When a resistive load is connected to a PV module, the operating point of the module (which is current and voltage output) is decided by intersection of the I–V characteristics curve of the PV module (which is modeled in Section 3) and the I–V characteristics of the load curve (which is determined from the famous simple electrical correlation, i.e., V=IR). According to the electrical correlation (i.e., V=IR), the slope of the load curve (which is straight line) is expressed as 1/R on I-V plane. The operating point will depend on the value of R (see Figure 5 for visual understanding) [12].

Figure 5 depicts that for smaller resistive load, as radiation intensity increases the operating point will move continuously towards the maximum power point (MPP) of each
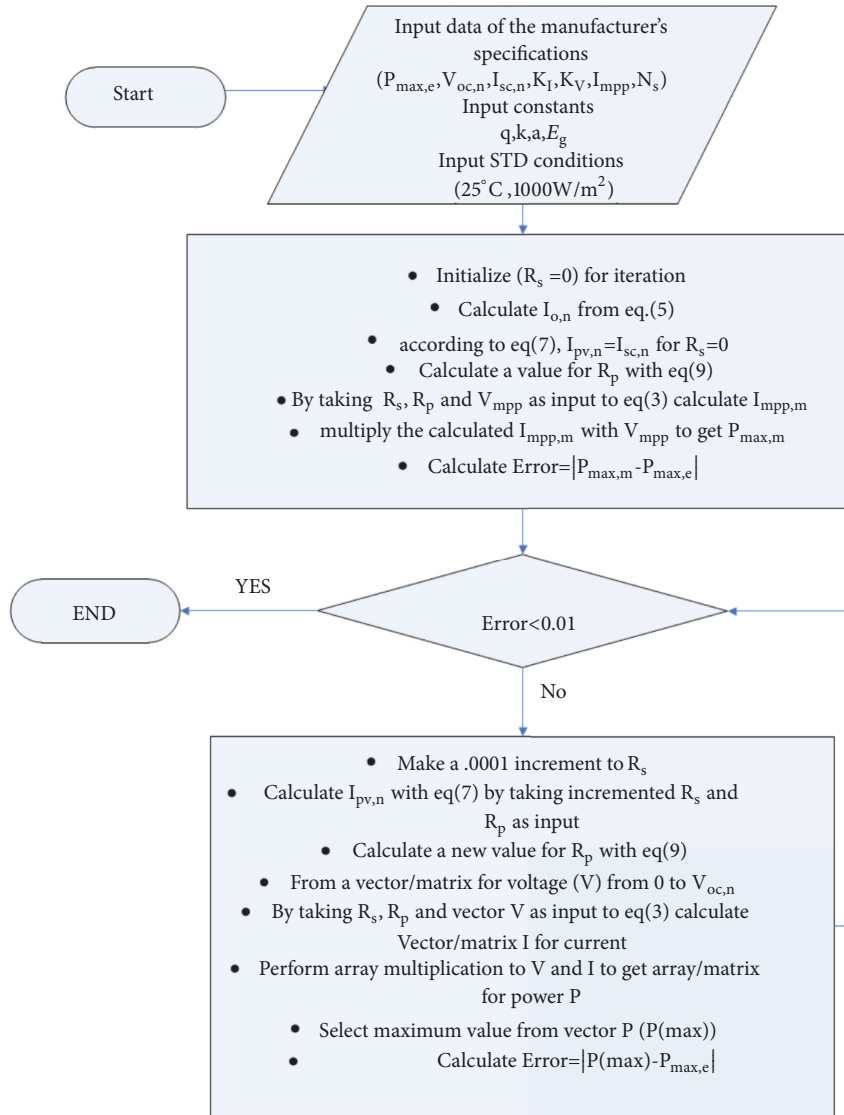
FIGURE 4: Algorithm of computer program used to model a PV panel.

6. Results and Discussion

curve as it is pointed by points A, B, and C; hence the efficiency will improve continuously. In the contrary, for higher resistive load the operating point will not move continuously towards the MPP, rather first it moves towards the MPP and then it moves away from the MPP as pointed by points D, E, and F. Hence the efficiency of the PV panel will first improve then it drops as radiation intensity continuously increases.

6. Results and Discussion

Here in this paper we are modeling a particular PV module (which is Kyocera 200 GT) under constant electric load and weather condition of Jigjiga. Hence annual temperature and global radiation (i.e., pyranometer) data from Ethiopian

National Metrology Agency is provided which is measured in 15 minutes' difference.

6.1. Output Result of the Computer Program for Selected PV Module. A PV module is chosen as reference example for modeling, because it is well-suited to traditional applications of photovoltaics, which is KC200GT.

The proposed model was tested using manufacturer data sheets. Figures 6 and 7 show different simulations for a Kyocera family solar module using the information provided by the manufacturer KYOCERA, for the products KC200GT.

The I-V curves (which are shown in Figure 6) depict the simulation results for current versus voltage characteristics of the photovoltaic modules with the operating cell temperature of 25°C and the effective irradiance level changing (i.e.,
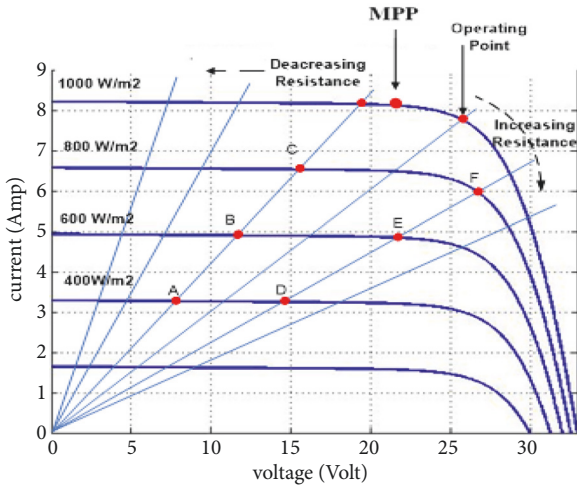
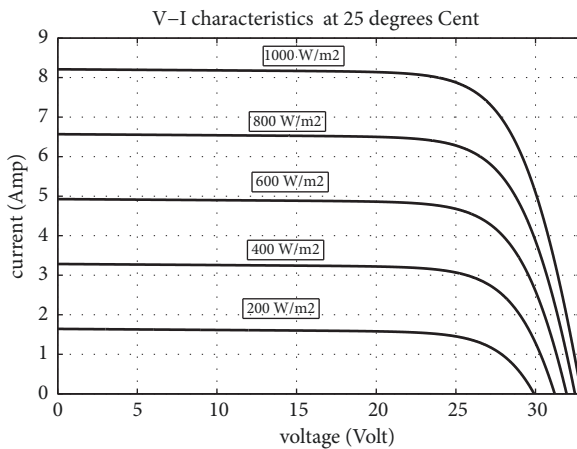FIGURE 5: Effect of resistive load on cell operating point.

FIGURE 7: P–V model curves of the KC200GT solar module at different irradiations, 25°C.

FIGURE 6: I–V model curves of the KC200GT solar module at different irradiations, 25°C.

FIGURE 8: I–V model curves of the KC200GT solar module at different temperature, 1000W/m^2.

$200W/m^2$, $400W/m^2$, $600W/m^2$, $800W/m^2$, and $1000W/m^2$). The figure showed the increase in short-circuit current of the PV panel with increase in radiation intensity. Similarly, the P-V curves (of Figure 7) show power versus voltage characteristics at different effective irradiance level and 25°C cell temperature. It showed the increase in maximum power output of the PV panel with increase in radiation intensity. It can be validated that I-V curve on Figure 6 and P-V curve of Figure 7 are very similar to the I-V and P-V curve plotted by *Marcelo G. et al.* [21].

Figure 8 show simulation results for I-V curve of the photovoltaic module KC200GT under different temperatures of operation (i.e., 25°C, 50°C, and 75°C) with the irradiation level at 1000W/m^2. The figure depicts insignificant rise in short-circuit current while a significant drop in open-circuit voltage of the PV panel with increase in cell temperature. Figure 9 shows the adverse effect of temperature to the maximum power supplied by the photovoltaic module under a constant irradiance level of 1000W/m^2.
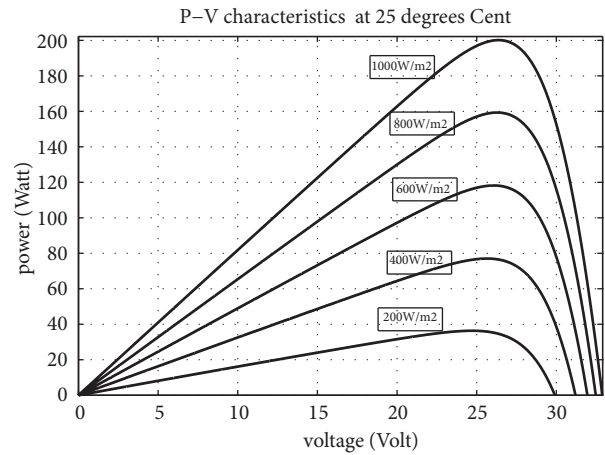

FIGURE 9: P–V model curves of the KC200GT solar module at different temperature, 1000W/m^2.
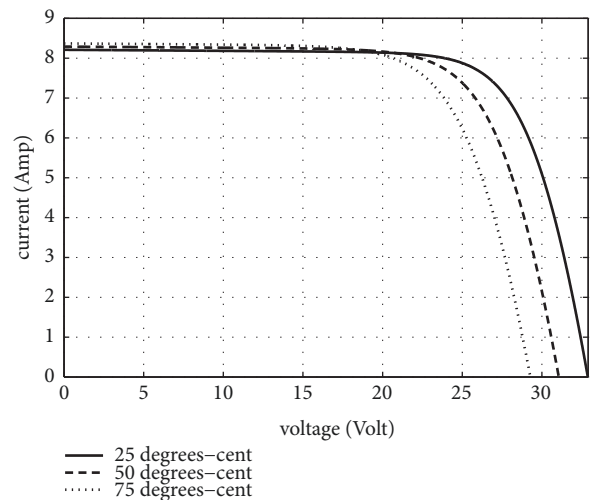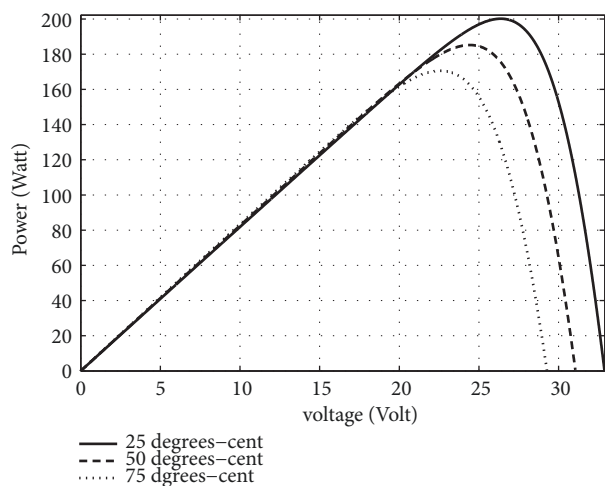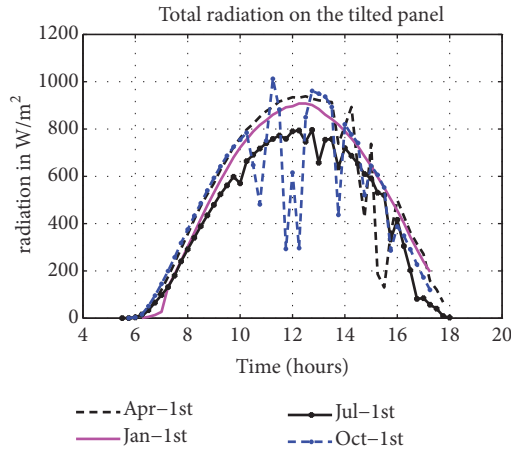
FIGURE 10: Hourly variation of global radiation on optimally tilted panel.

FIGURE 11: Hourly variation of PV module operating temperature.

6.2. Hourly Variation of Global Radiation on a Tilted Panel. Flat plate photovoltaic systems (like KC200GT) do not use focusing devices, so all three components—beam, diffuse, and reflected—can contribute to energy collected; hence we have to use the global radiation in the analysis of module temperature as well as power generation [25].

Total radiation intensity (i.e., global radiation) is measured with pyranometer, which measures radiation intensity on horizontal surface. However, facing a collector toward the equator (for our case, Jigjiga is at the Northern Hemisphere; this means facing it south) and tilting it up at an angle equal to the local latitude is a good rule-of-thumb for annual performance [25]; hence it will be convincing to tilt our system to its optimum angle (i.e., at an angle equal to the local latitude) and to perform the analysis based on the tilting angle. Figure 10 shows hourly variation of global or total radiation on the optimally tilted panel.

6.3. Hourly Variation of PV Module Operating Temperature. Equation (11) can model operating temperature of a PV module from NOCT and environmental variables (i.e., ambient temperature and radiation intensity). Figure 11 shows variation in operating temperature of the PV module for the the considered days (i.e., January 1st, April 1st, July 1st, and October 1st).

6.4. Hourly Variation of Electric Performance of the PV Module. This paper is concerned with modelling of a typical PV module (i.e., Kyocera 200GT), at constant electric load and under a weather condition of Jigjiga. Figures 12, 13, 14, and 15 depict hourly variation in voltage, current, power output, and conversion efficiency of the PV module for the first dates of selected months under 2Ω electric load.

For the 2Ω electric load as radiation increases, all the electrical characteristics (i.e., voltage, current, and power output as well as efficiency) will increase continuously and decrease when radiation intensity decreases. Because as radiation increases the operating point jumps from smaller I-V curve to higher I-V. Also, as it is mentioned in Section 5, for
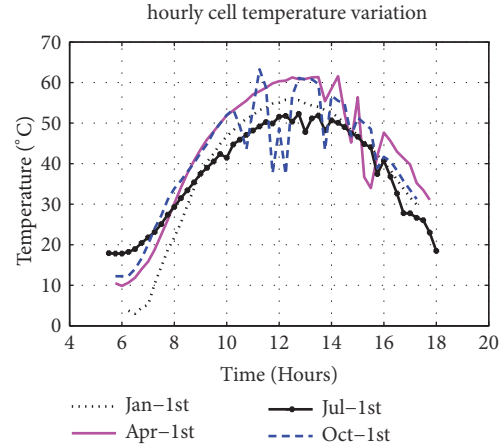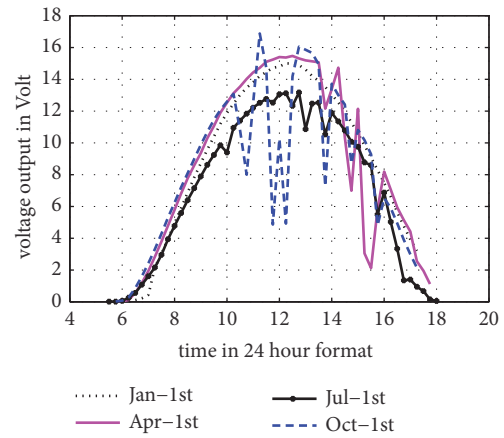

FIGURE 12: Hourly variation of voltage output of Kyocera 200GT PV module for 2Ω resistance.

smaller electric loads the operating point will continuously move towards maximum power point; hence the efficiency will improve continuously (refer to Figure 5).

6.5. Effect of Electric Load on Performance of the PV Panel. Figures 16 and 17 depict variation in electric performance of KC 200GT PV module for different electric load (i.e., 2Ω, 4Ω, 6Ω, and 8Ω electric resistance) and under weather condition of January 1st.

According to Figure 16, the 4Ω electric load caused a desirable efficiency. It resulted in a higher operating efficiency of the PV module for duration of the time at which the solar radiation intensity is the highest. This claim can be further inspected with Figure 17 (which shows hourly variation in power output of the PV module for different electric load). As it is depicted with the figure, the 4Ω electric load resulted in the highest power output from 10AM to 3PM time interval than other electric loads, the reason behind the scenario is that the PV panel operates relatively nearer to its maximum power point in the time interval when it is connected to the
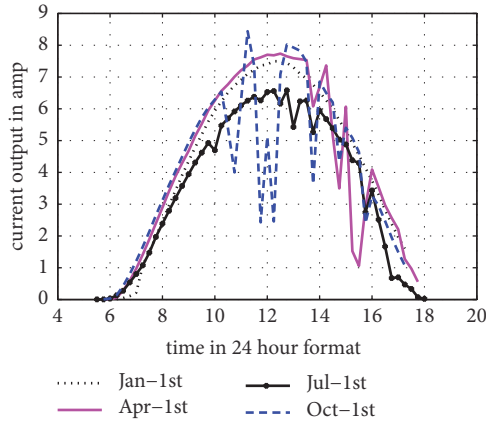
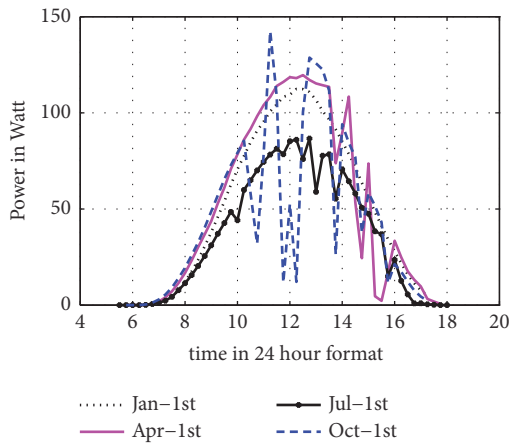Figure 13: Hourly variation of current output of Kyocera 200GT PV module for 2Ω resistance.

Figure 14: Hourly variation of power output of Kyocera 200GT PV module for 2Ω resistance.

Figure 15: Hourly variation of efficiency of Kyocera 200GT PV module for 2Ω resistance.

Figure 16: Hourly variation of efficiency of Kyocera 200GT PV module for different electric load under weather condition of January 1st.

4Ω. Then the 6Ω electric load has a better power output in the time interval next to the 4Ω electric load.

In addition, Figure 16 shows a u shape efficiency curve for 6Ω and 8Ω electric load for the time interval where radiation intensity is highest. This result asserts the concept stated in Section 5 that for higher resistive load the efficiency of the PV panel drops as the operating point moves beyond the maximum power point.

To judge the better performance of the PV module on the basis of electric load, the power output does not give us a clear picture. If an electric load gave as a better power output at some time interval, it does not mean that it performed better through all the time. Hence to have a clear picture, we have to compare the energy output of the PV module for each electric load. The following formula can help in the analysis of the daily energy output of the PV module. It calculates the areas under the curves of Figure 17:

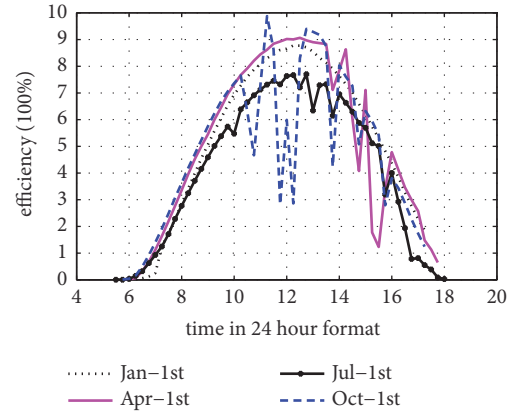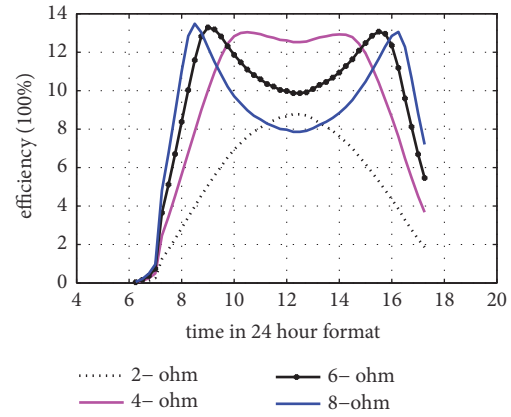$$E_{output} = \sum_{0:00}^{23:45} P_{out} \times \Delta t \qquad (13)$$

where E_{output} is daily energy output of the PV panel under an electric load, P_{out} is calculated power output, and Δt is time interval at which calculations are performed.

Figure 18 depicts daily energy output of the PV module for the first 12 days of the month of January under 2Ω, 4Ω, 6Ω, and 8Ω electric loads. According to the figure the 4Ω electric load resulted in the highest energy output among all other electric loads for the first 10 days of the month. In January 11th, it had the same amount of energy output as that of the 6Ω electric load, but in January 12th it is over taken by both 6Ω and 8Ω electric load. The 2Ω electric load had the lowest energy output than all other electric loads for all mentioned days of the month. The 2Ω electric load had the lowest energy output than all other electric load for all mentioned days of the month.

From this result it can be concluded that all environmental condition will not favor a single electric load all the time, but we can compare the annual performance of the PV module to judge which electric load will optimize the operation of the PV panel.
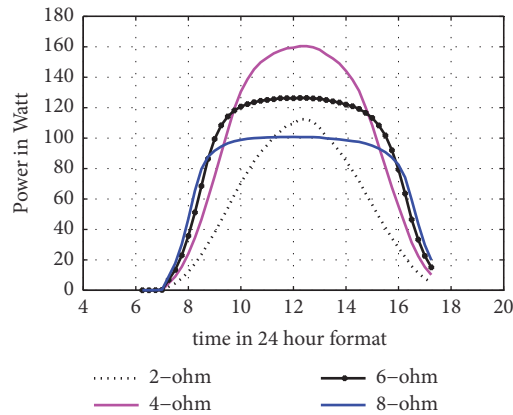
FIGURE 17: Hourly variation in power output of Kyocera 200GT PV module for different electric load under weather condition of January 1st.
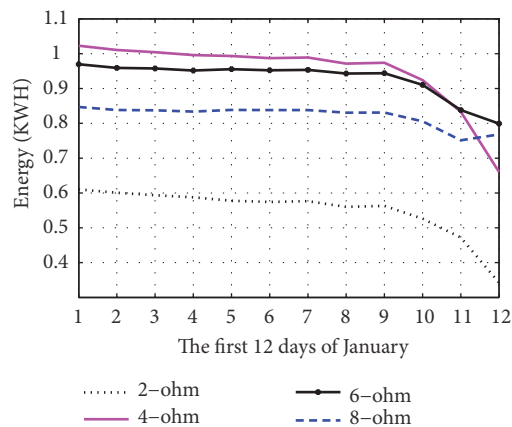

FIGURE 18: Variation in daily energy output of Kyocera 200GT PV module for the first 12 days of January under different electric load.

7. Conclusion and Recommendations

Most of previous research papers on solar PV system are concerned only with modelling the electrical characteristics of the PV system using a single-diode electrical model and investigated the effect of environmental parameters, which are radiation intensity and cell temperature on the performance of PV systems. In case of directly coupled PV system the electric load has also an effect on the performance of the PV system. Perhaps, resistor matching technique is one way of optimizing performance of a PV system. In this study, beside the environmental parameters, the effect of electrical loads on the performance of the PV system is investigated on real environmental parameter.

Based on tasted iterative technique (which is recommended by previous research papers), the modelling of a PV panel is performed. The hourly variation in electrical performance of a typical PV panel is simulated under real weather conditions. The performance of the PV panel is compared at different electrical loads. The 4Ω electric load resulted in the best operating performance of the PV panel on a daily basis for 11 days of the month of January (out of 12 days

on which measurements are taken for the month), but in the last day it resulted in the poorer performance with respect to the other two electrical loads (i.e., 6Ω and 8Ω electric loads). Hence it is concluded that every weather condition does not favor a single load all the time.

Data Availability

The Meteorological data used to support the findings of this study are included within the supplementary information file(s).

Conflicts of Interest

The authors declare that they have no conflict of interest regarding to the publication of this paper

Supplementary Materials

Description of Supplementary Material A supplementary material attached in this research is an Excel file for annual solar radiation and temperature data provided by Ethiopian National Meteorology agency which is used in the research *(Supplementary Materials)*

References

[1] A. A. W. Sayigh, *Renewable Energy*, Global Progress and Examples in Renewable Energy, Wren, 2001.

[2] T. B. Johansson, H. Kelly, A. K. N. Reddy, and R. H. Williams, "Renewable fuels and electricity for a growing world economy: defining and achieving the potential," *Energy Studies Review*, vol. 4, no. 3, 1993.

[3] A. Abu-Zour and S. Riffat, "Environmental and economic impact of a new type of solar louvre thermal collector," *International Journal of Low-Carbon Technologies*, vol. 1, no. 3, pp. 217–227, 2006.

[4] W. Charters, "Developing markets for renewable energy technologies," *Journal of Renewable Energy*, vol. 22, no. 1-3, pp. 217–222, 2001.

[5] K. Jagoda, R. Lonseth, A. Lonseth, and T. Jackman, "Development and commercialization of renewable energy technologies in Canada: An innovation system perspective," *Journal of Renewable Energy*, vol. 36, no. 4, pp. 1266–1271, 2011.

[6] J. M. Cansino, M. D. P. Pablo-Romero, R. Román, and R. Yñiguez, "Tax incentives to promote green electricity: an overview of EU-27 countries," *Energy Policy*, vol. 38, no. 10, pp. 6000–6008, 2010.

[7] R. E. H. Sims, H.-H. Rogner, and K. Gregory, "Carbon emission and mitigation cost comparisons between fossil fuel, nuclear and renewable energy resources for electricity generation," *Energy Policy*, vol. 31, no. 13, pp. 1315–1326, 2003.

[8] T. J. Dijkman and R. M. J. Benders, "Comparison of renewable fuels based on their land use using energy densities," *Renewable & Sustainable Energy Reviews*, vol. 14, no. 9, pp. X3148–3155, 2010.

 [9] P. D. Lund, "Effects of energy policies on industry expansion in renewable energy," *Journal of Renewable Energy*, vol. 34, no. 1, pp. 53–64, 2009.

[10] M. A. Eltawil and D. V. K. Samuel, "Vapor compression cooling system powered by solar PV array for potato storage," *Agricultural Engineering International: The CIGR E-Journal Manuscript*, vol. IX, 2007.

[11] E. F. Mba, J. L. Chukwuneke, C. H. Achebe, and P. C. Okolie, "Modeling and simulation of a photovoltaic powered vapor compression refrigeration system," *Journal of Information Engineering and Applications*, vol. 2, no. 10, 2012.

[12] Z. Salameh, *Renewable Energy System Design*, Elsevier Academic Press, 1st edition, 2014.

[13] S. S. Chandel, M. Nagaraju Naik, and R. Chandel, "Review of solar photovoltaic water pumping system technology for irrigation and community drinking water supplies," *Renewable & Sustainable Energy Reviews*, vol. 49, article no. 4338, pp. 1084–1099, 2015.

[14] G. Li, Y. Jin, M. Akram, and X. Chen, "Research and current status of the solar photovoltaic water pumping system – A review," *Renewable & Sustainable Energy Reviews*, vol. 79, pp. 440–458, 2017.

[15] B. Reshef, H. Suehrcke, and J. Appelbaum, "Analysis of a photovoltaic water pumping system," in *Proceedings of the 8th Convention on Electrical And Electronics Engineers in Israel*, pp. 7-8, 1995.

[16] B. Singh, C. P. Swamy, and B. Singh, "Analysis and development of a low-cost permanent magnet brushless DC motor drive for PV-array fed water pumping system," *Solar Energy Materials & Solar Cells*, vol. 51, no. 1, pp. 55–67, 1998.

[17] N. K. Lujara, J. D. van Wyk, and P. N. Materu, "Loss models of photovoltaic water pumping systems," in *Proceedings of the 5th IEEE AFRICON Conference (Electrotechnical Services for Africa)*, vol. 2, pp. 965–970, IEEE, 1999.

[18] A. A. Ghoneim, "Design optimization of photovoltaic powered water pumping systems," *Energy Conversion and Management*, vol. 47, no. 11-12, pp. 1449–1463, 2006.

[19] V. S. Gonal and G. S. Sheshadri, "Solar energy optimization using MPPT controller by maximum conductance method," in *Proceedings of the 7th IEEE Power India International Conference (PIICON)*, IEEE, India, 2016.

[20] A. Mengistu, *Agricultural Profile of Ethiopia from FAO*, http://www.fao.org/ag/agp/doc/pasture/forage.htm.

[21] V. Singla and V. K. Garg, "Modeling of solar photovoltaic module & effect of insolation variation using MATLAB/SIMULINK," *International Journal of Advanced Engineering Technology*, 2013.

[22] M. G. Villalva, J. R. Gazoli, and E. R. Filho, "Comprehensive approach to modeling and simulation of photovoltaic arrays," *IEEE Transactions on Power Electronics*, vol. 24, no. 5, 2009.

[23] R. Araneo, U. Grasselli, and S. Celozzi, "Assessment of a practical model to estimate the cell temperature of a photovoltaic module," *International Journal of Energy and Environmental Engineering*, 2014.

[24] A. Luqu and S. Hegedus, "Handbook of Photovoltaic Science and Engineerin," in *Sussex PO19 8SQ*, pp. 296-297, John Wiley & Sons Ltd, West Sussex, UK, 2003.

[25] G. M. Masters, *Electric Renewable and Efficient Power System*, John Wiley & Sons, 1st edition, 2004.